

Revealing the hydrogenated structure of silicene- $(\sqrt{13} \times \sqrt{13})R13.9^\circ$ by tip-induced dehydrogenation

Jinglan Qiu^{1,5,*}, Huimin Wang^{2,3}, Jing Wang^{1,6}, Xiaojing Yao^{1,6}, Sheng Meng^{2,3,4,†} and Ying Liu^{1,6}

¹College of Physics, Hebei Normal University, Shijiazhuang, Hebei 050024, China

²Beijing National Laboratory for Condensed Matter Physics and Institute of Physics, Chinese Academy of Sciences, Beijing 100190, China

³School of Physical Sciences, University of Chinese Academy of Sciences, Beijing 100190, China

⁴Songshan Lake Materials Laboratory, Dongguan, Guangdong 523808, China

⁵Hebei Key Laboratory of Photophysics Research and Application, Hebei Normal University, Shijiazhuang, Hebei 050024, China

⁶Hebei Advanced Thin Films Laboratory, Hebei Normal University, Shijiazhuang 050024, Hebei, China



(Received 18 August 2022; revised 23 October 2022; accepted 25 October 2022; published 2 November 2022)

The application of voltage pulse in a scanning tunneling microscope has been demonstrated to induce dehydrogenation on hydrogenated silicene/Ag(111), recovering intact silicene phases. This manipulation provides us a method to build a relationship between various silicene phases and their hydrogenated structures. Combining with density-functional theory calculations, hydrogenation of silicene- $(\sqrt{13} \times \sqrt{13})R13.9^\circ$ is found to produce the same half silicane as hydrogenated silicene- $(2\sqrt{3} \times 2\sqrt{3})R30^\circ$. These two silicene phases are suggested to be the same monolayer silicene on Ag(111), albeit with different Si buckling configurations and lattice strains. Our study not only reveals the hydrogenated structure of silicene- $(\sqrt{13} \times \sqrt{13})R13.9^\circ$, but also offers significant potential for lithography and modification of hydrogenated silicene at atomic scale for future design of silicene-based electronic devices.

DOI: [10.1103/PhysRevB.106.184102](https://doi.org/10.1103/PhysRevB.106.184102)

I. INTRODUCTION

As a monolayer two-dimensional silicon material, silicene possess a low-buckled honeycomb structure and presents Dirac cones near the Fermi level [1–4]. Due to the sp^2 - sp^3 hybridization of Si atoms, atoms and molecules are more favorable to adsorb on silicene than on graphene for chemical functionalization. Theoretically, hydrogenation of free-standing silicene is predicted to be a simple and effective method for tuning electronic properties of silicene by opening a band gap [5–7] and unraveling interesting ferromagnetic [6,8], optoelectronic [9], and thermoelectric [10] properties. Most of the experimental studies of silicene hydrogenation are focused on silicene phases grown on Ag(111) substrate, including (4×4) and $(2\sqrt{3} \times 2\sqrt{3})R30^\circ$ with respect to Ag(111)- (1×1) lattice. For example, reversible hydrogenation of silicene- (4×4) reveals an ordered structure with a sublattice adsorption mechanism by scanning tunneling microscope (STM) [11]. Raman investigations confirm that Si atoms undergo a rehybridization from a mixing sp^2 - sp^3 to a dominating sp^3 state and the hydrogenated silicene remains a two-dimensional nature [12]. In addition, the softening of Si-H vibrational modes of H/silicene- (4×4) is also studied by high-resolution electron-energy-loss spectroscopy [13]. For silicene- $(2\sqrt{3} \times 2\sqrt{3})R30^\circ$, the hydrogenated structure shows ordered half silicane with characteristic holes, following the same sublattice adsorption

mechanism with hydrogenation of silicene- (4×4) [14]. The band structure of half silicane is evidenced by angle-resolved photoelectron spectroscopy studies [15]. Besides silicene- (4×4) and $(2\sqrt{3} \times 2\sqrt{3})R30^\circ$, $(\sqrt{13} \times \sqrt{13})R13.9^\circ$ is another commonly observed silicene superstructure on Ag(111) [16–21], which is also suggested to be a continuous monolayer silicene by atomic force microscopy [22]. To fully understand the hydrogenation mechanism of silicene on Ag(111), the atomic structure of hydrogenated silicene- $(\sqrt{13} \times \sqrt{13})R13.9^\circ$ phase is worth studying.

Apart from hydrogenation, dehydrogenation where hydrogen atoms are desorbed or removed from surface, is also an important subject in tuning structural and electronic properties. By using the interactions present in the tunnel junction of STM, atoms and molecules can be manipulated in various ways [23,24]. A benefit from this technique, controlled dehydrogenation, which is also called hydrogen lithography (HL), has been used to create atomic-scale logic devices [25], quantum computing platforms [26], and single-atom transistors [27]. For hydrogenated silicene- (4×4) [11] and $(2\sqrt{3} \times 2\sqrt{3})R30^\circ$ structure [14], annealing to about 450 K has been demonstrated as an easy approach to induce dehydrogenation, recovering clean silicene phases on Ag(111). This fact suggests a large potential to realize hydrogen manipulation in hydrogenated silicene through STM.

In this paper, we demonstrate that by applying a voltage pulse (above +4.0 V) between STM tip and hydrogenated silicene, hydrogen atoms desorb from surface, recovering clean and intact silicene superstructures on Ag(111). The sizes of hydrogen desorption area increase with the raising of voltage pulses. This STM tip-induced dehydrogenation helps

*jlqiu@hebtu.edu.cn

†smeng@iphy.ac.cn

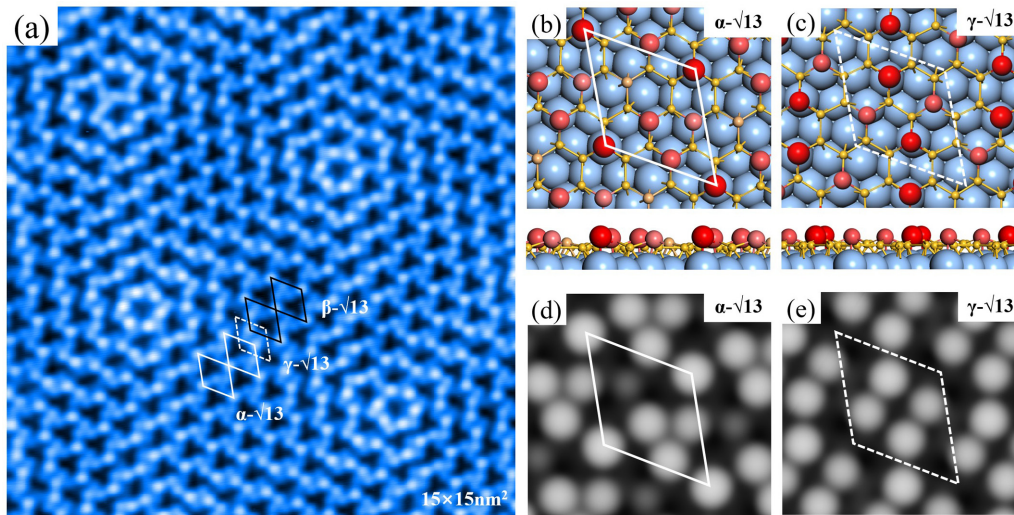


FIG. 1. STM image and structural model of silicene- $(\sqrt{13} \times \sqrt{13})R13.9^\circ$. (a) STM image ($I = 190.0$ pA, $U = +40.0$ mV) of silicene- $(\sqrt{13} \times \sqrt{13})R13.9^\circ$ shows vortexlike features formed by three phases: α - $\sqrt{13}$, β - $\sqrt{13}$, and γ - $\sqrt{13}$, whose unit cells are marked by white (solid line), black (solid line), and white (dotted line) rhombuses, respectively. (b), (c) Structural models of α - $\sqrt{13}$ and γ - $\sqrt{13}$. (d), (e) Simulated STM images of α - $\sqrt{13}$ and γ - $\sqrt{13}$.

us to establish a relationship between the hydrogenated silicene structures and the original silicene phases. Interestingly, the hydrogenated structure of silicene- $(\sqrt{13} \times \sqrt{13})R13.9^\circ$ is found to be exactly the same as the half silicane formed by H/silicene- $(2\sqrt{3} \times 2\sqrt{3})R30^\circ$ with similar hydrogenated mechanism confirmed by density-functional theory (DFT) calculations. These observations indicate that both silicene $(\sqrt{13} \times \sqrt{13})R13.9^\circ$ and silicene- $(2\sqrt{3} \times 2\sqrt{3})R30^\circ$ are complete monolayer silicene, albeit with different Si buckling configurations.

II. EXPERIMENTS AND METHODS

Our experiments were performed at a CreaTec molecular-beam epitaxy and low-temperature scanning tunneling microscopy system with a base pressure of about 4×10^{-11} mbar. The clean surface of Ag(111) single crystal was prepared by a few cycles of Ar^+ ion sputtering followed by annealing to about 900 K. Silicon atoms were evaporated by passing direct current through a silicon (Si) wafer to a temperature as high as 1300 K. During Si evaporation, Ag(111) substrate was held at about 500 K. Hydrogen atoms were achieved by cracking high-purity hydrogen gas (pressure: 1×10^{-6} mbar) with a hot tungsten filament heated to about 2000 K. When performing hydrogen adsorption, silicene/Ag(111) sample was maintained at room temperature (about 300 K). The experiments of STM tip-induced hydrogen desorption were carried out at liquid nitrogen temperature (77 K) under constant-current feedback control. The bias voltage was defined as the sample bias with respect to the tip.

The calculations were performed using DFT as implemented in the Vienna *Ab initio* Simulation Package (VASP) [28] with the Perdew-Burke-Ernzerhof exchange-correlation functional [29] and projector-augmented wave pseudopotentials. The plane-wave basis set with an energy cutoff at 350 eV was applied. In the calculation, the $(\sqrt{7} \times \sqrt{7})$ supercells of silicon film on the five-layer $(\sqrt{13} \times \sqrt{13})R13.9^\circ$ Ag (111)

surface with the lattice constant of 10.42 \AA were chosen. The vacuum region of $>15 \text{ \AA}$ in the surface-normal direction is sufficiently large to eliminate artificial interactions between periodic images. All the structures were fully relaxed with the bottom two layers of Ag atoms fixed. The Brillouin zone is sampled by $5 \times 5 \times 1$ Monkhorst-Pack k mesh. Geometry optimization was carried out until the residual force on each atom was less than 0.04 eV/\AA .

III. RESULTS AND DISCUSSION

The STM image and structural model of the commonly reported silicene- $(\sqrt{13} \times \sqrt{13})R13.9^\circ$ are shown in Fig. 1. In the large-scale image of Fig. 1(a), silicene- $(\sqrt{13} \times \sqrt{13})R13.9^\circ$ presents characteristic vortexlike features formed by combination of three phases: α - $\sqrt{13}$, β - $\sqrt{13}$, and γ - $\sqrt{13}$ [17]. In α - $\sqrt{13}$ phase, there are four protrusions inside its unit cell (UC) and one big protrusion in the corner of UC marked by white rhombus in the structural model of Fig. 1(b) and the simulated STM image of Fig. 1(d). Among the four protrusions, three brighter ones form a trimer in the lower-half unit cell (HUC), while another dark one locates in the middle of the upper HUC. β - $\sqrt{13}$ is the inverted phase of α - $\sqrt{13}$. γ - $\sqrt{13}$ is also called defected line or domain wall [22]. Its UC is marked by white rhombus (dotted line) in Fig. 1(a), which connects both α - $\sqrt{13}$ and β - $\sqrt{13}$. From the structural model and simulated image of γ - $\sqrt{13}$ in Figs. 1(c) and 1(e), we can find a typical square pattern that contains four protrusions. In the STM image, two protrusions in one diagonal are found to be brighter than those other two in the other diagonal.

Silicene- $(\sqrt{13} \times \sqrt{13})R13.9^\circ$ always coexists with (4×4) and even $(2\sqrt{3} \times 2\sqrt{3})R30^\circ$ phases, depending on the substrate temperature and silicon coverage [30]. In this experiment, all of the above three silicene phases form multiphase silicene on Ag(111) and are fully hydrogenated. One patch of the hydrogenated structure with bright

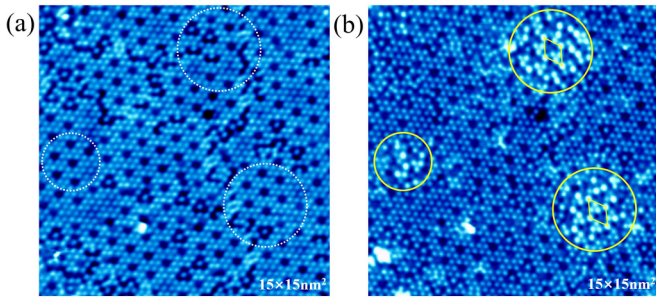


FIG. 2. STM voltage pulses induce dehydrogenation from hydrogenated silicene surface. (a) High-resolution image ($I = 200.8$ pA, $U = -51.5$ mV) of hydrogenated silicene ($I = 200.8$ pA, $U = +300.0$ mV) before applying voltage pulses. White circles (dotted line) mark the locations where voltage pulses are applied. (b) Same area as (a) after applying voltage pulses (left middle: +4.9 V, right up: +7.9 V, right down: +7.9 V). Yellow circles (solid line) mark the locations where dehydrogenation occurs.

hydrogenated spots and characteristic holes is shown in Fig. 2(a). In STM, applying voltage pulses between tip and sample is a normal tip-poking procedure to obtain a sharp tip for high-resolution images. Occasionally, we find that suitable voltage pulses are able to induce some significant changes on hydrogenated silicene/Ag(111) surface. During the constant-current scanning mode, when a small voltage pulse of about +3.2 V (setpoint: 200 pA, 500 mV) is applied on surface, no change is found. Raising the pulses to higher than +4.0 V, changes start to happen. Since a typical voltage pulse ($I = 200$ pA, $t = 10^{-3}$ s) contains approximately 10^6 electrons, the silicon and hydrogen (Si-H) bond energy of 3.5 eV [31] should be compared with the energy of single tunneling electron. Dehydrogenation occurs when the energy of single tunneling electron is larger than Si-H bond energy.

To precisely understand the influence of voltage pulse on hydrogenated silicene, we gradually increase the controlled voltage pulses from 0 to 10 V. Three examples of controlled voltage pulses have been applied above three different locations marked by white circles (dotted line) in Fig. 2(a). The resulting surface of the same locations after tip pluses is presented in Fig. 2(b). In the left middle of Fig. 2(a), a +4.9-V pulse induces dehydrogenation and creates an area of about (2×2) square nanometers. Some of the resulting protrusions in Fig. 2(b) look bigger and brighter than the original hydrogenated spots. Apparently, it is difficult to determine which structure it is according to such a small hydrogen-terminated area. When we gradually raise the pulse voltage, the size of the dehydrogenated area also increases. Two individual +7.5-V pulses are applied separately above the two locations on the right side of Fig. 2(a). Obviously, much larger patches of hydrogen-free area [about (3.2×3.2) square nanometers] are created than at +4.9 V. Closer inspection of these two patches in Fig. 2(b) reveals two ordered areas with two inverted unit cells. Comparing with the original silicene phases on Ag(111), it is exciting to find that the upper-right one and the lower-right one look like the unit cells of α - $\sqrt{13}$ and β - $\sqrt{13}$, respectively, in silicene- $(\sqrt{13} \times \sqrt{13})R13.9^\circ$ [17]. These atomic-scale observations confirm again the dehydrogenation induced by STM voltage

pulses. Moreover, it indicates that dehydrogenation appears to convert hydrogenated silicene structure to original silicene phases on Ag(111).

According to our previous investigations, hydrogenated silicene- (4×4) shows an ordered γ - (4×4) [11], while hydrogenated $(2\sqrt{3} \times 2\sqrt{3})R30^\circ$ presents half silicene with hexagonal close-packed (hcp) silicene- (1×1) spots, characteristic holes, and domain boundaries [14]. Different silicene phases on Ag(111) result in different hydrogenated structures. Since the hydrogenated structure in Fig. 2(a) looks nearly the same as the above half silicene, at first glance, we would naturally consider that it is formed by hydrogenation of silicene- $(2\sqrt{3} \times 2\sqrt{3})R30^\circ$ [14]. However, the obtained α - $\sqrt{13}$ and β - $\sqrt{13}$ after dehydrogenation in Fig. 2(b) are parts of silicene- $(\sqrt{13} \times \sqrt{13})R13.9^\circ$. This means that it is possible for silicene- $(\sqrt{13} \times \sqrt{13})R13.9^\circ$ to share the same hydrogenated structure as silicene- $(2\sqrt{3} \times 2\sqrt{3})R30^\circ$. To prove it, all characteristics of silicene- $(\sqrt{13} \times \sqrt{13})R13.9^\circ$ should be observed after dehydrogenation, including the three phases and the vortexlike features. However, the sizes of hydrogen-terminated areas in Fig. 2(b) are too small to precisely determine their corresponding silicene phase.

To solve this problem, a simple measure we can take is to apply repeated voltage pulses on a large hydrogenated area to induce a large amount of hydrogen desorption. Before the application of voltage pulses, full access to the details of hydrogenated structure is needed. Figure 3(a) shows a large area of homogeneous hydrogenated silicene with a small area of Ag(111) substrate in the lower-left corner. In the zoom-in high-resolution images of Figs. 3(b) and 3(c), more detailed characteristics are resolved, including the hcp protrusions with a lattice period of about 3.8 Å, similar as silicene- (1×1) lattice, and three types of characteristic holes (mono-, double-, and triple hole). The monoholes present a short-range ordered structure with a period of about 10.2 Å, corresponding to the superstructure of Si- $(\sqrt{7} \times \sqrt{7})$ with respect to silicene- (1×1) lattice, which is marked by the red rhombus in Fig. 3(c). Besides, a small number of double holes and triple holes [marked by yellow ellipse and yellow circle, respectively, in Fig. 3(c)] distribute sporadically on surface. It should be noted that the bright hcp protrusions in Fig. 3(b) are not continuous; instead, they are separated into three domains by domain boundaries marked by irregular yellow dotted lines. These structures are nearly the same as our previously reported half silicene on hydrogenated silicene- $(2\sqrt{3} \times 2\sqrt{3})R30^\circ$.

When placing the STM tip above the location marked by the yellow irregular shape (dotted line) in Fig. 3(a) and applying more than six repeated voltage pulses of +7.5 V on it, a large amount of hydrogen atoms desorb from surface, resulting in a large area of clean silicene that shows characteristic vortexlike features of silicene- $(\sqrt{13} \times \sqrt{13})R13.9^\circ$ in Fig. 3(d) [17,19,21,22]. Closer inspection of the zoom-in high-resolution images in Figs. 3(e) and 3(f) reveals three silicene- $(\sqrt{13} \times \sqrt{13})R13.9^\circ$ phases, including α - $\sqrt{13}$, β - $\sqrt{13}$, and γ - $\sqrt{13}$ [17], whose UCs are marked by white (solid line), black (solid line), and white (dotted line), respectively, in Fig. 3(f). Obviously, all of the above features observed after dehydrogenation coincide with those in silicene- $(\sqrt{13} \times \sqrt{13})R13.9^\circ$ shown in Fig. 1 [17]. This suggests

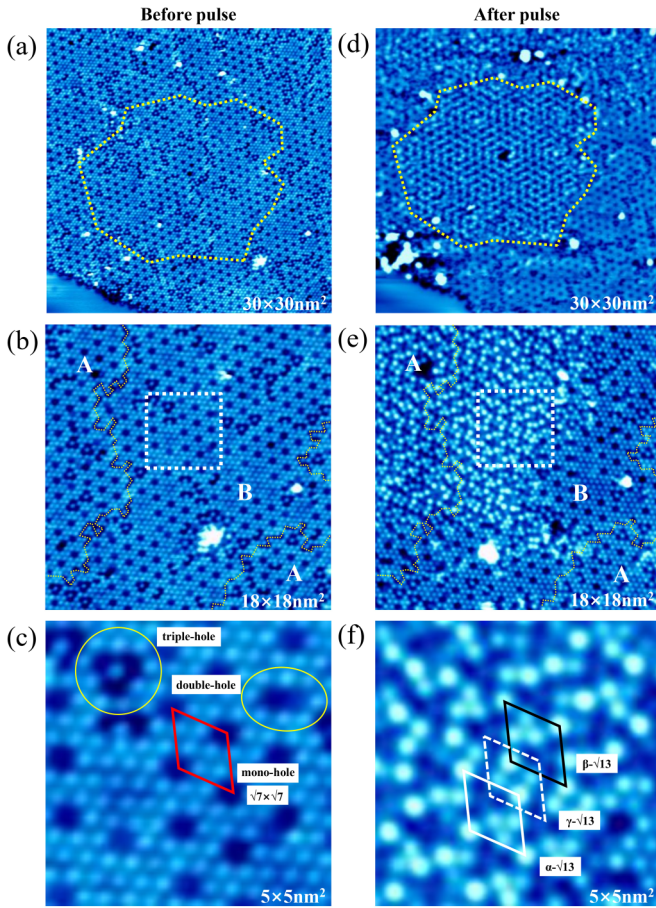


FIG. 3. STM voltage pulse induces dehydrogenation from hydrogenated silicene surface. (a) ($I = 200.8$ pA, $U = -51.5$ mV) and (d) ($I = 200.8$ pA, $U = +50.0$ mV) Large-scale STM image of fully hydrogenated silicene before and after voltage pulses. (b) ($I = 200.8$ pA, $U = +51.5$ mV) and (e) ($I = 200$ pA, $U = +515.7$ mV) Zoom-in images of (a) and (d). The letters A and B mark the two sublattices of silicene. Domain boundaries are marked by the irregular yellow dotted lines. (c) ($I = 200.8$ pA, $U = +51.5$ mV) and (f) ($I = 200.8$ pA, $U = +515.7$ mV) Zoom-in high resolution images of the area marked by white dashed squares in (b) and (e). The red rhombus represents the unit cell of short-range ordered monoholes. Double hole and triple hole are marked, respectively, by the yellow ellipse and circle. (f) Unit cells of α - $\sqrt{13}$, β - $\sqrt{13}$, and γ - $\sqrt{13}$ are marked by white (solid line), black (solid line), and white (dotted line) rhombuses, respectively.

that STM voltage pulse induces an atomic-scale conversion from hydrogenated silicene to silicene- $(\sqrt{13} \times \sqrt{13})R13.9^\circ$ through hydrogen desorption.

Since the multiphase silicene sample we have grown contains both $(\sqrt{13} \times \sqrt{13})R13.9^\circ$ and $(2\sqrt{3} \times 2\sqrt{3})R30^\circ$ phases, it is natural to expect that we should be able to get silicene- $(2\sqrt{3} \times 2\sqrt{3})R30^\circ$ phase through the application of STM voltage pulses. By moving the scanning tip, we apply voltage pulses in various locations and check every structure after dehydrogenation. Figure 4(a) shows one of the hydrogenated structures before applying controlled voltage pulses. Similar hcp silicene- (1×1) spots and three types of characteristic holes can be found as those in Fig. 3(c). However, there

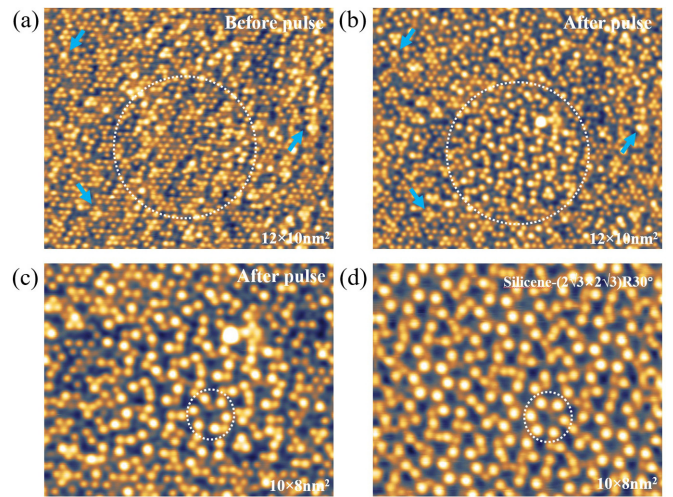


FIG. 4. STM tip-induced dehydrogenation on hydrogenated silicene- $(2\sqrt{3} \times 2\sqrt{3})R30^\circ$. (a) ($I = 207.0$ pA, $U = +400.0$ mV) and (b) ($I = 400.0$ pA, $U = +207.0$ mV) Large-scale STM images of hydrogenated silicene before and after voltage pulses that are applied in the area marked by white circle (dotted line). Blue arrows mark the features that are totally the same in the two images, indicating the same location. (c) Zoom-in high-resolution image ($I = 400.0$ pA, $U = +207.0$ mV) shows the characteristic perfect honeycomb marked by white circle (dotted line) and the surrounding defected hexagons in silicene- $(2\sqrt{3} \times 2\sqrt{3})R30^\circ$. (d) High-resolution image ($I = 400.0$ pA, $U = -4.7$ mV) of silicene- $(2\sqrt{3} \times 2\sqrt{3})R30^\circ$, which shows the characteristic perfect honeycomb and defected hexagons.

are some extra-bright protrusions which make the surface a bit disordered. In Fig. 2, we have shown that the protrusions after dehydrogenation are presented with higher density of states and look much brighter than the other hydrogenated spots in the STM image. Hence, these extra protrusions in Fig. 4(a) are considered as some hydrogen-free silicon atoms that come from some individual hydrogen desorption cases triggered by the application of voltage pulses during scanning nearby. After the application of repeated voltage pulses (about $+7.5$ V) above the area surrounded by white circle (dotted line) in Fig. 4(a), dehydrogenation results in a totally different silicene structure [Fig. 4(b)] from the vortexlike features shown in Fig. 3(d). High-resolution image of Fig. 4(c) reveals the characteristic perfect honeycomb and the surrounding defected hexagons, which are the same as silicene- $(2\sqrt{3} \times 2\sqrt{3})R30^\circ$ before hydrogenation [Fig. 4(d)]. This experiment confirms that STM voltage pulse can also induce an atomic-scale conversion from half silicene to silicene- $(2\sqrt{3} \times 2\sqrt{3})R30^\circ$ through hydrogen desorption.

From the experimental results of Fig. 3 and Fig. 4, silicene- $(\sqrt{13} \times \sqrt{13})R13.9^\circ$ and silicene- $(2\sqrt{3} \times 2\sqrt{3})R30^\circ$ are found to produce the same half silicene after hydrogenation. In the following, we perform DFT calculations to understand more deeply the formation of half silicene by hydrogenation of silicene- $(\sqrt{13} \times \sqrt{13})R13.9^\circ$. The silicene α - $\sqrt{13}$ phase shown in Figs. 5(a) and 5(f) is chosen as an example to present the calculations. When considering the two sublattices of silicene, we can find from Fig. 5(a) that the four Si atoms of both

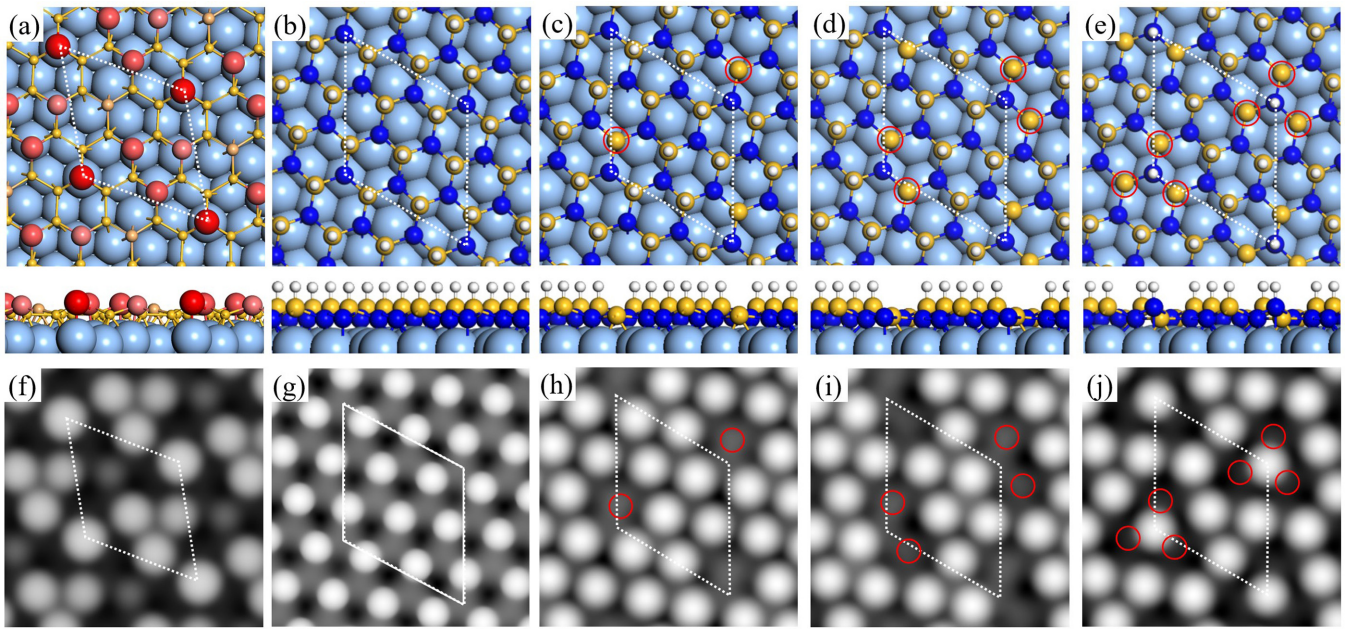


FIG. 5. DFT calculations of the formation of hydrogenated silicene- (1×1) spots and three types of characteristic holes. (a) Structural model of silicene $\alpha\text{-}\sqrt{13}$ phase. (b) Structural model of perfect half silicene formed by hydrogenation of silicene $\alpha\text{-}\sqrt{13}$, in which the yellow sublattice of silicene is fully hydrogen terminated. (c)–(e) The mono-, double-, and triple-hole structures formed by one, two, or three Si atoms without hydrogenation, respectively. The hydrogen-unbonded yellow Si atoms are marked by red circles. (f)–(j) Corresponding simulated STM images of (a)–(e).

the trimer and the dark spot inside the UC belong to the same sublattice (marked by yellow sublattice), while the corner protrusion belongs to the other one (marked by blue sublattice). If the yellow sublattice in Fig. 5(b) is fully hydrogen terminated, a perfect silicene- (1×1) lattice is obtained in the simulated STM image of Fig. 5(g). Actually, in Fig. 3(b), we can find some very small patches of such a perfect area. However, most of the hydrogenated structure in Figs. 3(a)–3(c) are not perfect silicene- (1×1) lattice. Evidenced by hydrogenation of silicene- $(2\sqrt{3} \times 2\sqrt{3})R30^\circ$, the long-range ordered perfect silicene- (1×1) is not the most stable hydrogenated structure [14]. Therefore, the observed half silicane presents characteristic hole features and domain boundaries. The calculated results in Figs. 5(c)–5(e) show that when one, two, or three yellow Si atoms (marked by red circles) nearest to the corner blue Si atom are hydrogen unbonded, the mono-, double-, and triple-hole features are formed.

The detailed formation mechanism of these characteristic holes is related to the “sublattice adsorption picture” and the buckling change of Si atoms during hydrogenation. The sublattice adsorption picture has been demonstrated in our previous work of hydrogenated silicene- (4×4) and $(2\sqrt{3} \times 2\sqrt{3})R30^\circ$ [11,14] that there is the same possibility for the two different sublattices of silicene to be hydrogenated [14]. Following this mechanism, half silicane is found to be separated by domain boundaries. Each domain corresponds to hydrogenation of one silicene sublattice. In Fig. 3(b), the domain boundaries marked by irregular yellow lines are clearly observed. A zoom-in domain boundary is highlighted in Fig. 6(a). When superimposing the honeycomb silicene lattice with two sublattices across the domain boundary in Fig. 6(a), the hydrogenated protrusions in the left domain are

found to coincide with the blue sublattice, while the protrusions in the right domain match perfectly with the yellow sublattice. Here, the two sublattices of silicene are marked by A and B. From many large-scale images of hydrogenated silicene like Fig. 3(a), we find that the area sizes of the two domains formed by hydrogenated A- or B sublattice are nearly the same. Therefore, the sublattice adsorption picture also works well in hydrogenated silicene- $(\sqrt{13} \times \sqrt{13})R13.9^\circ$.

The formation of characteristic holes can be explained as follows. Since hydrogen bonding changes the buckling of Si atoms from mixing sp^2 - sp^3 to sp^3 [12], when the yellow

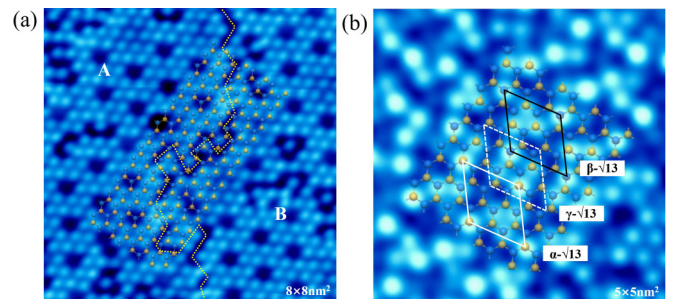


FIG. 6. Superimposing the silicene lattice (a) across the domain boundary of hydrogenated silicene ($I = 200.8$ pA, $U = +51.5$ mV) and (b) on the three phases of silicene- $(\sqrt{13} \times \sqrt{13})R13.9^\circ$ ($I = 200.8$ pA, $U = +51.7$ mV). (a) Blue and yellow sublattices of silicene- (1×1) coincide with the protrusions in the left and right domains, respectively. (b) Unit cells of $\alpha\text{-}\sqrt{13}$, $\beta\text{-}\sqrt{13}$, and $\gamma\text{-}\sqrt{13}$ in STM image are marked by white (solid line), black (solid line), and white (dotted line) rhombuses, respectively. They match well with the continuous silicene lattice.

sublattice is hydrogen terminated, the corner blue Si atom in the UC is hydrogen unbonded and pushed downward [Fig. 5(b)]. On the contrary, its three nearest yellow Si atoms should be hydrogen bonded and buckle up [Fig. 5(b)]. However, these three yellow Si atoms possess the lowest buckling in original silicene- $(\sqrt{13} \times \sqrt{13})R13.9^\circ$. It is thus difficult for them to be totally hydrogen bonded and buckle up during hydrogenation. Eventually, one, two, or three of these Si atoms are found to be hydrogen unbonded, resulting in mono-, double-, and triple-hole features. It is worth noting that for triple hole, when the three nearest yellow Si atoms are all hydrogen unbonded, the middle blue Si atom is bonded with a hydrogen atom and appears as a protrusion. During STM scanning, there is no specific bias voltage for imaging H-unbonded Si atoms as dark-hole features. This phenomenon is different from the H-unterminated Si atoms on silicon surface like Si(100), which look bright because of their dangling bonds remained [31]. It is supposed that the above difference may come from the low buckled atomic structure of silicene and the interaction between silicene and Ag(111) surface. The structural models and simulated STM images of these hole features are shown in Figs. 5(c)–5(e) and Figs. 5(h)–5(j), in which the red circles mark the hydrogen-unbonded Si atoms of yellow sublattice. The above formation mechanism of characteristic holes is also similar to hydrogenated silicene- $(2\sqrt{3} \times 2\sqrt{3})R30^\circ$ [14].

In the above discussions, we have demonstrated from experimental results and DFT calculations that silicene- $(2\sqrt{3} \times 2\sqrt{3})R30^\circ$ and silicene- $(\sqrt{13} \times \sqrt{13})R13.9^\circ$ share the same hydrogenated structures, producing the same half silicane. In fact, there are also some important relationships of lattice geometries and strains between these two phases. Both silicene- $(\sqrt{13} \times \sqrt{13})R13.9^\circ$ and silicene- $(2\sqrt{3} \times 2\sqrt{3})R30^\circ$ are named relative to Ag(111)- (1×1) . If referring to silicene- (1×1) , they are indeed Si layers with $(\sqrt{7} \times \sqrt{7})$ structures lying on Ag(111) substrate, albeit with different Si buckling configurations. However, due to the lattice mismatch between Si layer and Ag(111) substrate, the Si- $(\sqrt{7} \times \sqrt{7})$ structures possess different local strains. According to Pflugradt *et al.*'s calculations in 2014 [32], Si- $(\sqrt{7} \times \sqrt{7})$ /Ag- $(2\sqrt{3} \times 2\sqrt{3})R30^\circ$ possesses the largest compressive strain of 1.25%, while in Si- $(\sqrt{7} \times \sqrt{7})$ /Ag- $(\sqrt{13} \times \sqrt{13})R13.9^\circ$, a tensile biaxial strain of -2.79% is predicted. Considering the lattice strain, Jamgotchian *et al.* suggested that when applying contraction stress in silicene- $(2\sqrt{3} \times 2\sqrt{3})R30^\circ$, a periodic relaxation of the strain will result in periodic defective areas located around perfect $(2\sqrt{3} \times 2\sqrt{3})R30^\circ$ areas; similarly, the expansion stress in silicene- $(\sqrt{13} \times \sqrt{13})R13.9^\circ$ gives rise to the vortexlike superstructure [19,33]. Since the bonding of hydrogen atoms changes the hybridization of Si atoms in silicene from mixing sp^2 - sp^3 to sp^3 , together with the formation of hydrogenated silicene- (1×1) lattice, the lattice strains are released, resulting in characteristic holes. From this point of view, it is understandable that no matter compressive or tensile strain, hydrogenated silicene- $(\sqrt{13} \times \sqrt{13})R13.9^\circ$ and $(2\sqrt{3} \times 2\sqrt{3})R30^\circ$ produce similar half silicane. These findings can be also supported by energetics of strained silicene decorated by H atoms demonstrated in Ref. [34] that tensile

(-2.79%) and compressive ($+1.25\%$) strains lead to almost identical binding energies of H atoms on silicene.

In Fig. 6(b), silicene- (1×1) honeycomb lattice has been superimposed on the obtained silicene- $(\sqrt{13} \times \sqrt{13})R13.9^\circ$ after dehydrogenation. We can obviously find that the protrusions of α - $\sqrt{13}$, β - $\sqrt{13}$, and γ - $\sqrt{13}$ in STM image match well with the continuous silicene lattice. Combining with the formation of half silicane and the discussions of lattice strains, we suggest that silicene- $(\sqrt{13} \times \sqrt{13})R13.9^\circ$ and $(2\sqrt{3} \times 2\sqrt{3})R30^\circ$ are essentially the same monolayer silicene on Ag(111), albeit with different Si buckling configurations. Although silicene- $(2\sqrt{3} \times 2\sqrt{3})R30^\circ$ shows higher thermal stability than silicene- $(\sqrt{13} \times \sqrt{13})R13.9^\circ$, when choosing appropriate substrate temperature and Si coverage, they can also coexist on the same surface.

In this work, we have demonstrated the ability of STM tip-induced dehydrogenation on hydrogenated silicene. A threshold voltage of about $+4.0$ V is found for hydrogen desorption. To realize future hydrogen lithography on half silicane down to the atomic scale, the detailed mechanism of dehydrogenation is worth to be resolved. In fact, the STM-induced desorption of hydrogen from hydrogenated silicon surfaces, like H/Si(111) and H/Si(100) system, have been intensively studied with two hydrogen desorption mechanisms: electronic and vibrational excitations [35,36]. Considering the similarities of Si–H bonding nature, we suppose that the hydrogen desorption from half silicane may also be attributed to the above two mechanisms. Limited by our experimental results, detailed discussions about the dehydrogenation mechanism are unavailable in this paper. We expect that more future experimental and theoretical investigations will be focused on this subject.

IV. CONCLUSION

In summary, we have demonstrated that dehydrogenation is able to be induced by STM voltage pulses higher than $+4.0$ V, converting half silicane to intact silicene phases on Ag(111). Through this method, it is found that the hydrogenation of both silicene- $(\sqrt{13} \times \sqrt{13})R13.9^\circ$ and silicene- $(2\sqrt{3} \times 2\sqrt{3})R30^\circ$ results in similar half-silicane structure, containing silicene- (1×1) lattice and three types of characteristic holes. DFT calculations and the discussions of lattice strain evidence the formation of half silicane and suggest that both silicene- $(\sqrt{13} \times \sqrt{13})R13.9^\circ$ and silicene- $(2\sqrt{3} \times 2\sqrt{3})R30^\circ$ are essentially the same monolayer silicene on Ag(111). This work not only reveals the hydrogenated structure of silicene- $(\sqrt{13} \times \sqrt{13})R13.9^\circ$, but also provides a method to manipulate and modify half silicane down to the atomic scale for future device applications.

ACKNOWLEDGMENTS

This work was supported by the National Natural Science Foundation of China (Grants No. 11604075 and No. 12174084), the Natural Science Foundation of Hebei Province (Grants No. A2017205122 and No. A2021205024), and China Postdoctoral Science Foundation (Grants No. BX201700068 and No. 2017M620095).

- [1] K. Takeda and K. Shiraishi, Theoretical possibility of stage corrugation in Si and Ge analogs of graphite, *Phys. Rev. B* **50**, 14916 (1994).
- [2] C. C. Liu, W. Feng, and Y. Yao, Quantum Spin Hall Effect in Silicene and Two-Dimensional Germanium, *Phys. Rev. Lett.* **107**, 076802 (2011).
- [3] Y. Feng, D. Liu, B. Feng, X. Liu, L. Zhao, Z. Xie, Y. Liu, A. Liang, C. Hu, Y. Hu, S. He, G. Liu, J. Zhang, C. Chen, Z. Xu, L. Chen, K. Wu, Y.-T. Liu, H. Lin, Z.-Q. Huang, C.-H. Hsu, F.-C. Chuang, A. Bansil, and X. J. Zhou, Direct evidence of interaction-induced Dirac cones in a monolayer silicene/Ag(111) system, *Proc. Natl. Acad. Sci.* **113**, 14656 (2016).
- [4] B. Feng, H. Zhou, Y. Feng, H. Liu, S. He, I. Matsuda, L. Chen, E. F. Schwier, K. Shimada, S. Meng, and K. Wu, Superstructure-induced Splitting of Dirac Cones in Silicene, *Phys. Rev. Lett.* **122**, 196801 (2019).
- [5] L. Voon, E. Sandberg, R. S. Aga, and A. A. Farajian, Hydrogen compounds of group-IV nanosheets, *Appl. Phys. Lett.* **97**, 163114 (2010).
- [6] P. Zhang, X. D. Li, C. H. Hu, S. Q. Wu, and Z. Z. Zhu, First-principles studies of the hydrogenation effects in silicene sheets, *Phys. Lett. A* **376**, 1230 (2012).
- [7] S. Y. Lin, S. L. Chang, N. T. T. Tran, P. H. Yang, and M. F. Lin, H-Si bonding-induced unusual electronic properties of silicene: A method to identify hydrogen concentration, *Phys. Chem. Chem. Phys.* **17**, 26443 (2015).
- [8] F. B. Zheng and C. W. Zhang, The electronic and magnetic properties of functionalized silicene: A first-principles study, *Nanoscale Res. Lett.* **7**, 422 (2012).
- [9] B. Huang, H.-X. Deng, H. Lee, M. Yoon, B. G. Sumpter, F. Liu, S. C. Smith, and S.-H. Wei, Exceptional Optoelectronic Properties of Hydrogenated Bilayer Silicene, *Phys. Rev. X* **4**, 021029 (2014).
- [10] Y. F. Li, G. H. Tang, and B. Fu, Hydrogenation: An effective strategy to improve the thermoelectric properties of multilayer silicene, *Phys. Rev. B* **99**, 235428 (2019).
- [11] J. Qiu, H. Fu, Y. Xu, A. I. Oreshkin, T. Shao, H. Li, S. Meng, L. Chen, and K. Wu, Ordered and Reversible Hydrogenation of Silicene, *Phys. Rev. Lett.* **114**, 126101 (2015).
- [12] D. Solonenko, V. Dzhagan, S. Cahangirov, C. Bacaksiz, H. Sahin, D. R. T. Zahn, and P. Vogt, Hydrogen-induced sp^2 - sp^3 rehybridization in epitaxial silicene, *Phys. Rev. B* **96**, 235423 (2017).
- [13] D. B. Medina, E. Salomon, G. Le Lay, and T. Angot, Hydrogenation of silicene films grown on Ag(111), *J. Electron Spectrosc. Relat. Phenom.* **219**, 57 (2017).
- [14] J. Qiu, H. Fu, Y. Xu, Q. Zhou, S. Meng, H. Li, L. Chen, and K. Wu, From silicene to half-silicene by hydrogenation, *ACS Nano* **9**, 11192 (2015).
- [15] W. Wang, W. Olovsson, and R. I. G. Uhrberg, Band structure of hydrogenated silicene on Ag(111): Evidence for half-silicene, *Phys. Rev. B* **93**, 081406(R) (2016).
- [16] H. Jamgotchian, Y. Colignon, N. Hamzaoui, B. Ealet, J. Y. Hoarau, B. Aufray, and J. P. Bibérian, Growth of silicene layers on Ag(111): Unexpected effect of the substrate temperature, *J. Phys.: Condens. Matter* **24**, 172001 (2012).
- [17] Z.-L. Liu, M.-X. Wang, J.-P. Xu, J.-F. Ge, G. L. Lay, P. Vogt, D. Qian, C.-L. Gao, C. Liu, and J.-F. Jia, Various atomic structures of monolayer silicene fabricated on Ag(111), *New J. Phys.* **16**, 075006 (2014).
- [18] H. Enriquez, S. Vizzini, A. Kara, B. Lalmi, and H. Oughaddou, Silicene structures on silver surfaces, *J. Phys.: Condens. Matter* **24**, 314211 (2012).
- [19] H. Jamgotchian, B. Ealet, H. Maradj, J. Y. Hoarau, J.-P. Bibérian, and B. Aufray, A comprehensive analysis of the $(\sqrt{13} \times \sqrt{13})R13.9^\circ$ type II structure of silicene on Ag(111), *J. Phys.: Condens. Matter* **28**, 195002 (2016).
- [20] L. Feng, K. Yabuoshi, Y. Sugimoto, J. Onoda, M. Fukuda, and T. Ozaki, Structural identification of silicene on the Ag(111) surface by atomic force microscopy, *Phys. Rev. B* **98**, 195311 (2018).
- [21] M. R. Tchalala, H. Enriquez, H. Yildirim, A. Kara, A. J. Mayne, G. Dujardin, M. A. Ali, and H. Oughaddou, Atomic and electronic structures of the $(\sqrt{13} \times \sqrt{13})R13.9^\circ$ of silicene sheet on Ag(111), *Appl. Surf. Sci.* **303**, 61 (2014).
- [22] R. Pawlak, C. Drechsel, P. D'Astolfo, M. Kisiel, E. Meyer, and J. I. Cerda, Quantitative determination of atomic buckling of silicene by atomic force microscopy, *Proc. Natl. Acad. Sci.* **117**, 228 (2020).
- [23] D. M. Eigler and E. K. Schweizer, Positioning single atoms with a scanning tunnelling microscope, *Nature (London)* **344**, 524 (1990).
- [24] A. A. Tseng and Z. Li, Manipulations of atoms and molecules by scanning probe microscopy, *J. Nanosci. Nanotechnol.* **7**, 2582 (2007).
- [25] T. Huff, H. Labidi, M. Rashidi, L. Livadaru, T. Dienel, R. Achal, W. Vine, J. Pitters, and R. A. Wolkow, Binary atomic silicon logic, *Nat. Electron.* **1**, 636 (2018).
- [26] L. Livadaru, P. Xue, Z. Shaterzadeh-Yazdi, G. A. DiLabio, J. Mutus, J. L. Pitters, B. C. Sanders, and R. A. Wolkow, Dangling-bond charge qubit on a silicon surface, *New J. Phys.* **12**, 083018 (2010).
- [27] M. Fuechle, J. A. Miwa, S. Mahapatra, H. Ryu, S. Lee, O. Warschkow, L. C. L. Hollenberg, G. Klimeck, and M. Y. Simmons, A single-atom transistor, *Nat. Nanotechnol.* **7**, 242 (2012).
- [28] G. Kresse and J. Furthmüller, Efficient iterative schemes for *ab initio* total-energy calculations using a plane-wave basis set, *Phys. Rev. B* **54**, 11169 (1996).
- [29] J. P. Perdew, K. Burke, and M. Ernzerhof, Generalized Gradient Approximation Made Simple, *Phys. Rev. Lett.* **77**, 3865 (1996).
- [30] K.-H. Wu, A review of the growth and structures of silicene on Ag(111), *Chin. Phys. B* **24**, 086802 (2015).
- [31] L. Soukiassian, A. J. Mayne, M. Carbone, and G. Dujardin, Atomic-scale desorption of H atoms from the Si(100)-2 \times 1:H surface: Inelastic electron interactions, *Phys. Rev. B* **68**, 035303 (2003).
- [32] P. Pflugradt, L. Matthes, and F. Bechstedt, Silicene-derived phases on Ag(111) substrate versus coverage: *Ab initio* studies, *Phys. Rev. B* **89**, 035403 (2014).
- [33] B. E. H. Jamgotchian, Y. Colignon, H. Maradj, J.-Y. Hoarau, J.-P. Bibérian, and B. Aufray, A comprehensive study of the $(2\sqrt{3} \times 2\sqrt{3})R30^\circ$ structure of silicene on Ag(111), *J. Phys.: Condens. Matter* **27**, 395002 (2015).

- [34] A. Podsiadły-Paszkowska and M. Krawiec, Electrical and mechanical controlling of the kinetic and magnetic properties of hydrogen atoms on free-standing silicene, *J. Phys.: Condens. Matter* **28**, 284004 (2016).
- [35] R. S. Becker, G. S. Higashi, Y. J. Chabal, and A. J. Becker, Atomic-scale Conversion of Clean Si(111): $H-1 \times 1$ to Si(111)- 2×1 by Electron-Stimulated Desorption, *Phys. Rev. Lett.* **65**, 1917 (1990).
- [36] T. C. Shen, C. Wang, G. C. Abeln, J. R. Tucker, J. W. Lyding, P. Avouris, and R. E. Walkup, Atomic-scale desorption through electronic and vibrational excitation mechanisms, *Science* **268**, 1590 (1995).